RESOURCE GEOLOGY

doi: 10.1111/rge.12014 *Resource Geology* Vol. 63, No. 4: 350–359

Original Article

Fluid Inclusion and Stable Isotope Studies at Don Sixto, a Precious Metal Low Sulfidation Deposit in Mendoza Province, Argentina

Ana Cecilia Mugas Lobos and María Florencia Márquez-Zavalía

IANIGLA, CCT Mendoza-CONICET, Mendoza, Argentina

Abstract

The Don Sixto mining area in Mendoza province, central-western Argentina, contains an epithermal low sulfidation Au–Ag deposit. It is a small deposit (~4 km^2), with a gold resource of 36 t. In Don Sixto, ore minerals are disseminated in the hydrothermal quartz veins and hydrothermally altered volcanic-pyroclastic rock units of Permian–Triassic age. On the basis of the texture, ore mineral paragenesis and cross cutting relationship of gangue minerals, seven stages of mineralization were recognized and described. The first six stages are characterized by quartz veins with minor amounts of base metal minerals and the last stage is represented by fluorite veins with minimal quantities of base metal minerals; the precious metal mineralization is mainly related to the fourth stage. The hydrothermal veins exhibit mainly massive, crustiform and comb infilling textures; the presence of bladed quartz replacement textures and quartz veins with adularia crystals are indicative of boiling processes in the system. Fluid inclusion and complementary stable isotope studies were performed in quartz, fluorite, and pyrite samples from the vein systems. The microthermometric data were obtained from primary, biphasic (liquid-vapor) fluid inclusion assemblages in quartz and fluorite. The maximum values for salinity and homogenization temperature (T_h) came from the stage IV where quartz with petrographic evidence of boiling has average values of 4.96 wt% $NaCl_{equiv.}$ and 286.9°C respectively. The lower values are related to the last stage of mineralization, where the fluid inclusions in fluorite have average salinities of 1.05 wt% $NaCl_{equiv.}$ and average homogenization temperatures of 173.1°C. The oxygen and sulfur isotopic fractionation was analyzed in quartz and pyrite. The calculated isotopic fractionation for oxygen in the hydrothermal fluid is in the range of $\delta^{18}O_{H2O}$ = –6.92 up to –3.08‰, which indicates dominance of a meteoric source for the water, while sulfur reaches $\delta^{34}S_{H2S}$ = 1.09‰, which could be reflecting a possible magmatic, or even a mixed source.

Keywords: bladed quartz, epithermal, fluid inclusions, low sulfidation, precious metals, stable isotopes.

1. Introduction

The Don Sixto mining area is one of the few epithermal precious metal deposits related to the Permian–Triassic magmatism, the Choiyoi Group, in central western Argentina. Don Sixto is a low sulfidation Au–Ag deposit with a gold resource of 36 t (Van der Heyden *et al.*, 2007). Antecedents in the area are scarce, the alteration halo of Don Sixto was first pointed out in 1996 while doing a Landsat imagery exploration and since then, surface geology and geochemistry studies were performed and more than 20,000 m have been

Received 2 November 2012. Accepted for publication 31 January 2013.
Corresponding author: A.C. Mugas Lobos, CCT Mendoza-CONICET, Av. Ruíz Leal S/N, Parque General San Martín—C.C. 330 (CP. 5500) Mendoza, Argentina. Email: amugas@mendoza-conicet.gob.ar

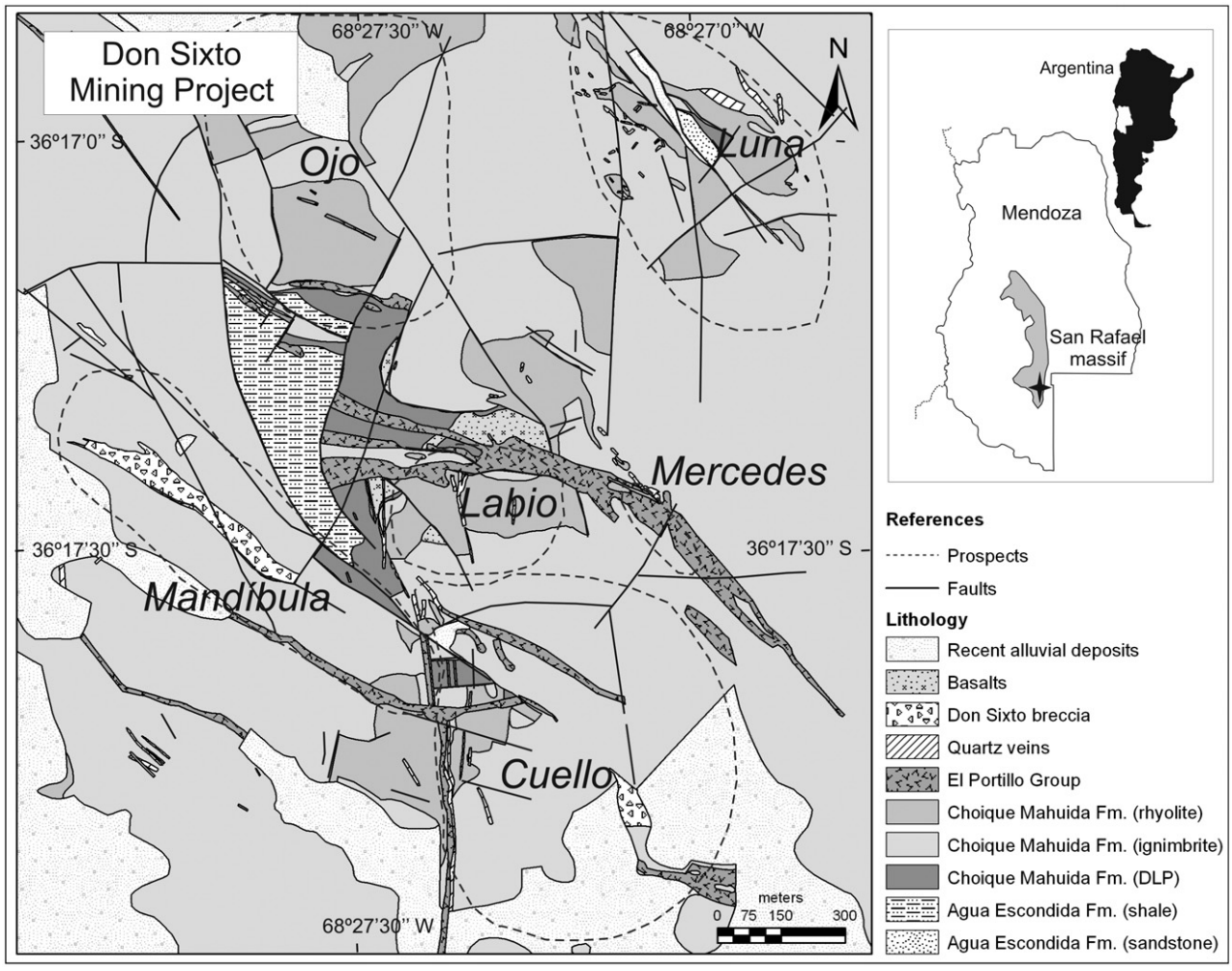

Fig. 1 Geological map of the Don Sixto mining area (Mugas Lobos *et al*., 2010; modified from Delendatti & Williams, 2007 and Van der Heyden *et al*., 2007).

drilled by the mining company. Previous works on this deposit, formerly known as El Pantanito o La Cabeza is scarce (Carpio *et al*., 2001; Rubinstein *et al*., 2001; Godeas & Rubinstein, 2004; Delendatti, 2005; Rubinstein & Gargiulo, 2005; Narciso *et al*., 2007). More recently, Mugas Lobos *et al*. (2010, 2011, 2012a, b) and Mugas Lobos (2012) give a complete description of the deposit. The main mineralized prospects or areas are: Cuello, Labio, Ojo, Luna, Mercedes, and Mandíbula (Fig. 1). On the basis of texture (Dong *et al*., 1995), ore mineral paragenesis and crosscutting relationship of gangue minerals, seven stages of mineralization were identified (Fig. 2).

From a metallogenetic point of view, the Choiyoi Group magmatism has been genetically linked to the formation of epithermal and transitional polymetallic mineralization (Zappettini, 1999), though in Chile, this magmatism is not related to significant mineralization. In Don Sixto area, the most abundant rocks belong to the Choique Mahuida Formation included in the upper section of Choiyoi Group, and El Portillo Group (Mugas Lobos *et al*., 2010). In this area (Fig. 1), the alteration-mineralization process has been recently dated by the $^{40}Ar/^{39}Ar$ multiple step heat method in adularia crystals; the resulting age 252.7 ± 1.3 Ma (Mugas Lobos, 2012) directly links the mineralization in the area to the local Permian–Triassic magmatism.

The aim of this contribution is to characterize this epithermal vein system, giving details about the gangue mineralogy, textures and temporal relationships. Microthermometric studies were performed and the results are discussed together with the stable

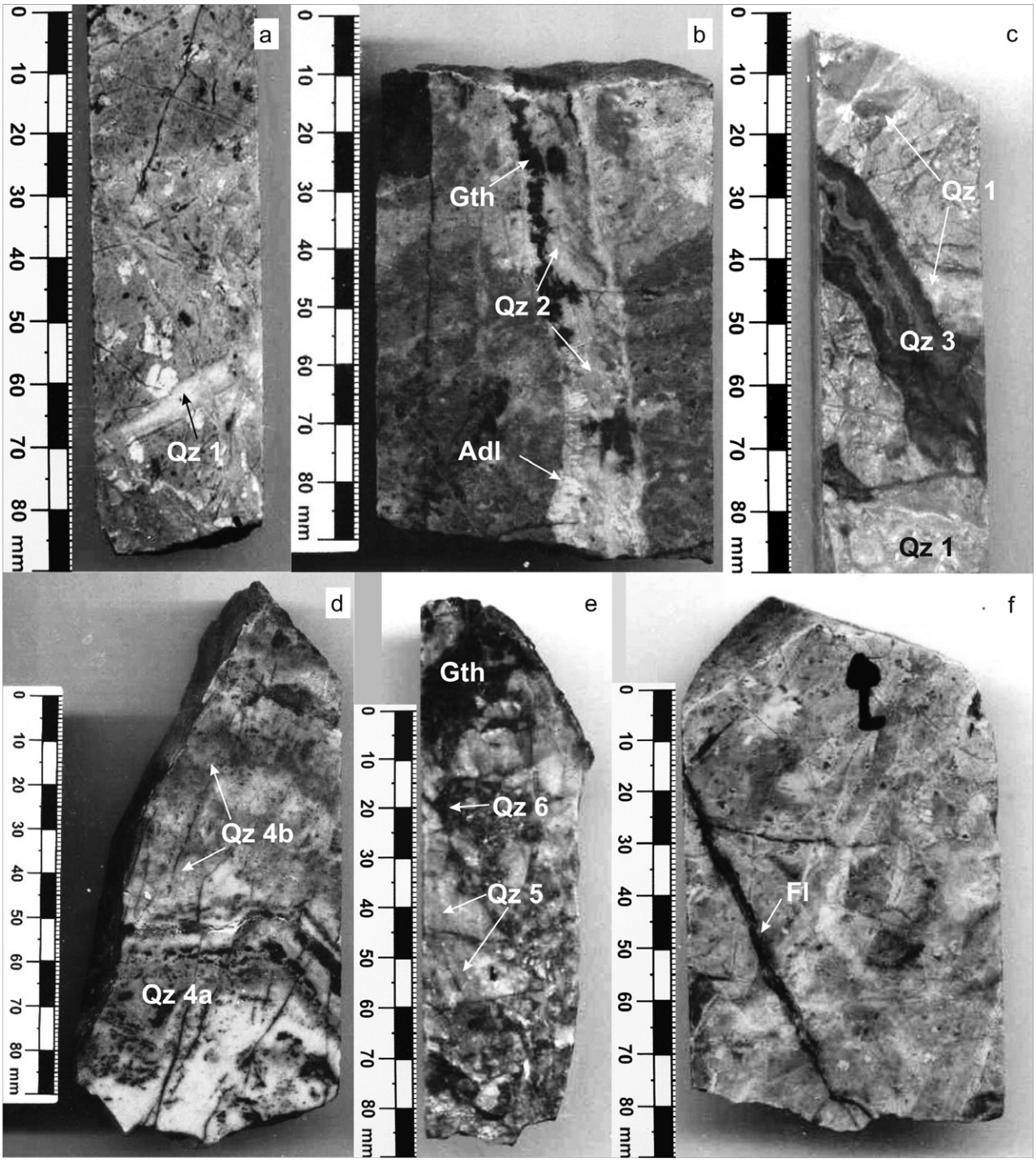

Fig. 2 (a) Quartz vein from Stage I. (b) Quartz–Adularia–Goethite (Qz–Adl–Gth) vein form Stage II. (c) Medium- to light-grey quartz vein from Stage III. (d) Banded structure in a vein from Stage IV. (e) Fragments of massive quartz from Stage V, cemented by dark-grey quartz, from Stage VI. (f) Thin veinlet of fluorite (Fl) from Stage VII. Mineral abbreviations after Whitney and Evans (2010).

isotope analyses, contributing to the understanding of the hydrothermal system in Don Sixto.

2. Geology

2.1 Regional background

Regarding the Gondwanic magmatism, during the Late Carboniferous–Early Permian to Triassic, widespread magmatism took place in northern and central Chile and Argentina; this plutonic-volcanic association has been known as the Choiyoi province (Kay *et al*., 1989) where the volcanic-pyroclastic sequences are associated with the Choiyoi Group in Argentina (Stipanicic *et al*., 1968) and the Pastos Blancos Group in Chile (Martin *et al*., 1999). Two different sections were identified in the Choiyoi Group: a lower section represented by andesite, dacite, and rhyolite, and an upper section, mainly rhyolitic (Llambías *et al*., 1993); the change in their composition reflects a change in the geotectonic environment. The genesis of these rocks was interpreted as typical of a transitional geotectonic environment, in between a volcanic arc and an intraplate post-orogenic distensive magmatic-tectonic environment (i.e. Kleiman, 1993; Llambías *et al*., 1993; Llambías, 1999; Ramos, 1999; Kleiman & Japas, 2009).

2.2 Local geology

In the Don Sixto mining area (Fig. 1), the marine clastic rocks of the Late Carboniferous Agua Escondida Formation are composed of alternating beds of sandstone and black to dark grey-bluish shale (Mugas Lobos *et al*., 2010). These rocks are uncomformably overlain by volcanic and pyroclastic sequences of the Lower Permian–Upper Triassic Choique Mahuida Formation, with rhyolite, rhyolitic ignimbrite, and pyroclastic lenticular deposits. Rhyolitic subvertical dikes of the Upper Permian–Lower Triassic El Portillo Group crosscut the previous sequences, mainly with a NW–SE and N–S strike. Two hydrothermal breccia bodies occur in the area: Don Sixto and Silicea. Both strike NW–SE, concordant with the major regional fault zones (Mugas Lobos, 2012). The Don Sixto breccia is red in color, composed of irregular fragments of quartz veins and altered volcanic rocks with minor partially limonitized sulfides, cemented by microcrystalline quartz with abundant limonite. The Silicea breccia is medium to dark grey colored, composed of irregular fragments of whitish grey quartz veins (1 to 3 cm) and minor strongly silicified volcanic rock fragments, with sericite, muscovite, and sulfides in the matrix, all cemented by microcrystalline quartz.

The volcanic and pyroclastic sequences are strongly to moderately silicified and moderately to strongly sericitized; argillic and propyllitic alteration is weak to moderate. The style of the gold mineralization is in quartz veins and disseminated in the volcanic-pyroclastic rock units of the Choique Mahuida Formation and El Portillo Group (Mugas Lobos *et al*., 2012a). The deposit is divided in six mineralized prospects: Cuello, Labio, Ojo, Luna, Mercedes, and Mandíbula (Fig. 1), which are nothing but different outcrops of the same vein system.

2.3 Vein system

The vein system occurs in an area with scattered outcrops of the mineralized prospects. Among the six main outcrop areas seven stages of mineralization were differentiated. The first one (Stage I; Qz 1) is well represented in most of the prospects. Quartz veins (Fig. 2a) are mainly massive, but also crustiform, colloform, and comb textures are locally present. This veins are light- to medium-grey colored and scarce pyrite and sericite may be present (QSP vein type).

Stage II (Qz 2) is mainly distributed in Labio, Mercedes, Cuello and Luna prospects (Fig. 2b). It is represented by thin (<2 cm wide), white to light grey crustiform, massive, bladed and cockade quartz + adularia veinlets with variable quantities of partially limonitized pyrite, 50 μm in size. The pinkish-orange adularia crystals are visible in hand specimen (size up to 3 mm); they have rhombic to sub-rhombic sections and pseudo-acicular habit. In many epithermal deposits, the presence of adularia has been considered a mineralogical indicator of boiling (Henley, 1985). Dong and Morrison (1995), on the bases of crystal habit, indicated that pseudo-acicular adularia (pseudomorph after carbonates) and rhombic adularia are commonly present in the epithermal veins; the former is found when extensive boiling is protracted. Nevertheless evidence of boiling was recognized in these veins, neither petrographic evidence was recognized in their fluid inclusions, nor was important precious metal mineralization present.

Stage III (Qz 3) is well represented in the same areas as Stage II; it is characterized by medium to dark grey quartz veins (<4 cm wide) with crustiform and comb textures with variable quantities of base metal sulfides and lesser sericite (Fig. 2c). The lack of adularia allows to easily differentiate between both stages.

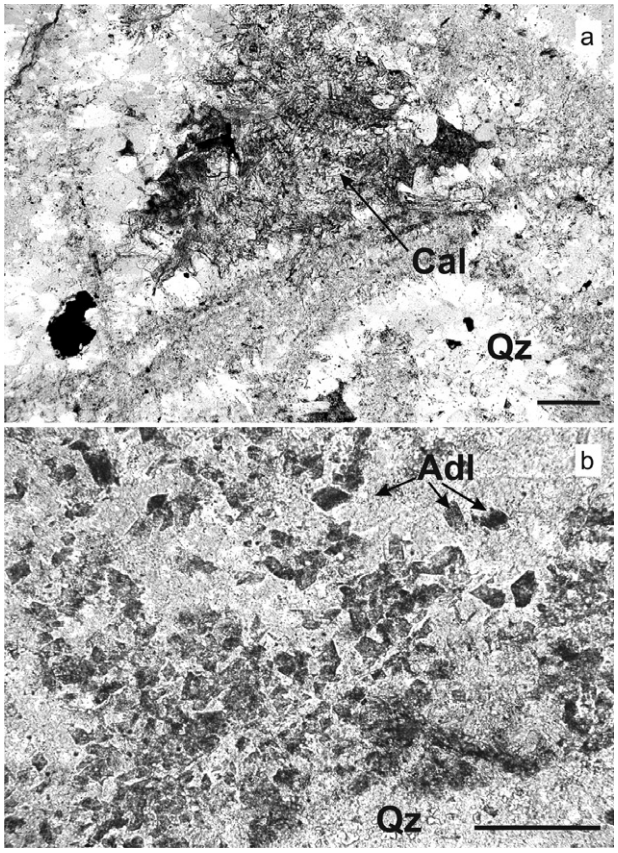

Fig. 3 (a) Lattice bladed quartz texture with calcite (Cal) as irregular and bladed crystals. (b) Rhombic adularia crystals (<60 μm) in a bladed quartz vein. Bar scale = 200 μm.

The veinlets of Stage IV are well distributed in the Cuello, Luna, and Labio prospects. Quartz veins are light- to medium-grey and the main textures are bladed quartz (Qz 4a), crustiform, massive (Qz 4b) and in some places banded (Fig. 2d). Occasionally, bladed quartz occurs together with bladed calcite (Fig. 3a), and/or rhombic adularia (Fig. 3b), which, following Dong and Morrison (1995), is an indication of extensive boiling. Other evidence, that also supports the presence of this process, is the boiling feature observed in the fluid inclusions associated with Qz 4a. The precious metal mineralization is mainly related to this stage, accompanied by variable quantities of partially oxidized sulfides.

In the Ojo and Mandíbula (OM) prospects, the Stage I of mineralization is identical to the rest of the deposit, Stage II is absent and Stages III and IV have special characteristics. Stage III-OM (Qz 3-OM) is represented by massive, light grey to white chalcedonic quartz veins with vugs and cavities, usually filled with limonite. In the Silicea breccia, fragments of these quartz veins are cemented by dark grey quartz with massive porous texture from the Stage IV-OM (Qz 4-OM). Sericite, partially limonitized pyrite, gold and lesser amounts of base metal sulfides are frequent.

Stage V (Qz 5) is characterized by light-grey to white massive quartz veins (Fig. 2e), with crustiform and comb textures, and variable amounts of chlorite and sulfides. These quartz veins are usually found as stockworks or cementing fragments of Qz 1, 2, 3, rhyolite and ignimbrite.

Stage VI (Qz 6) is characterized by the presence of medium- to dark-grey, massive quartz veins with abundant and partially limonitized pyrite and variable amounts of chlorite; it frequently cements fragments of quartz from Stages III and V (Fig. 2e) or develops veinlets and stockwork.

The last stage of the mineralization, Stage VII (Fl), is characterized by thin veinlets of massive purple-violet fluorite (Fig. 2f), scarce pyrite, quartz, calcite, and sericite. Fluorite veinlets are well represented in the Cuello prospect and may crosscut quartz veins from Stages IV and V.

3. Analytical methods

Microthermometric data were obtained with a Fluid Inc. adapted USGS gas-flow heating/freezing stage, mounted on a Leitz Laborlux transmitted light polarizing microscope from the Alfred Stelzner Museum (University of Córdoba, Córdoba, Argentina). The instrumental precision is ± 0.1°C between –56.6°C and 660.4°C, the data were always collected from primary, biphasic (liquid-vapor) inclusions in fluid inclusion assemblages (FIAs), and the salinities were indirectly obtained following Bodnar and Vityk (1994).

Stable isotope studies were performed at the Stable Isotope Research Facility (Indiana University, Bloomington, IN, USA). The oxygen fractionation $^{18}O/^{16}O$ was obtained by the Clayton and Mayeda (1963) method, with BrF_5; using as standards: Kan Pyx 9-14-11 I, Kan Pyx 9-14-11 J, EMR-Qtz 9-1-11 K, NCS-Qtz 8-27-11 M, NCS-Qtz 8-27-11 N, NCS-Qtz 9-1-11 M. The sulfur fractionation $^{34}S/^{32}S$ was obtained with a Costech 4010 EA element analyzer; using as standards: EMR-CP, ERE-Ag_2S, PQB_2, EMR-CP, ERE-Ag_2S, PQB_2, EMR-CP, ERE-Ag_2S, EMR-CP, PQB_2, ERE-Ag_2S. Corrected delta values are relative to VSMOW and VCDT, for oxygen and sulfur, respectively. The isotopic fractionation factors for quartz-H_2O and pyrite-H_2S were calculated in the

AlphaDelta website (Beaudoin & Therrien, 1999–2012). Zheng (1993) and Ohmoto and Rye (1979) equations were used for oxygen and sulfur respectively, together with the T_h of the corresponding stage of mineralization, followed by the $\delta^{18}O_{H2O}$ and $\delta^{34}S_{H2S}$ calculation.

4. Results

4.1 Fluid inclusion description

The microthermometric studies were performed in quartz and fluorite from drill cores to avoid reequilibration due to surface exposure (Bodnar, 2003). In Don Sixto, primary, pseudo-secondary and secondary fluid inclusions were recognized using the criteria of Roedder (1984) and Bodnar *et al*. (1985), and only primary fluid inclusions were used for microthermometric analyses. The latter are generally small (<10 μm), liquid rich, biphasic (liquid-vapor), and mainly irregular in shape; no carbonic phases were detected during microthermometric runs. The inclusions are arranged in groups, generally in the central part of the quartz crystals (Fig. 4a) or along the growth zones (Fig. 4b) where they are generally more abundant, although their size is generally smaller than the former. Evidence of boiling (Bodnar *et al*., 1985) was recognized in bladed quartz samples from Stage IV, where liquid-rich and vapor-rich fluid inclusions coexist in the same fluid inclusion assemblages (FIAs).

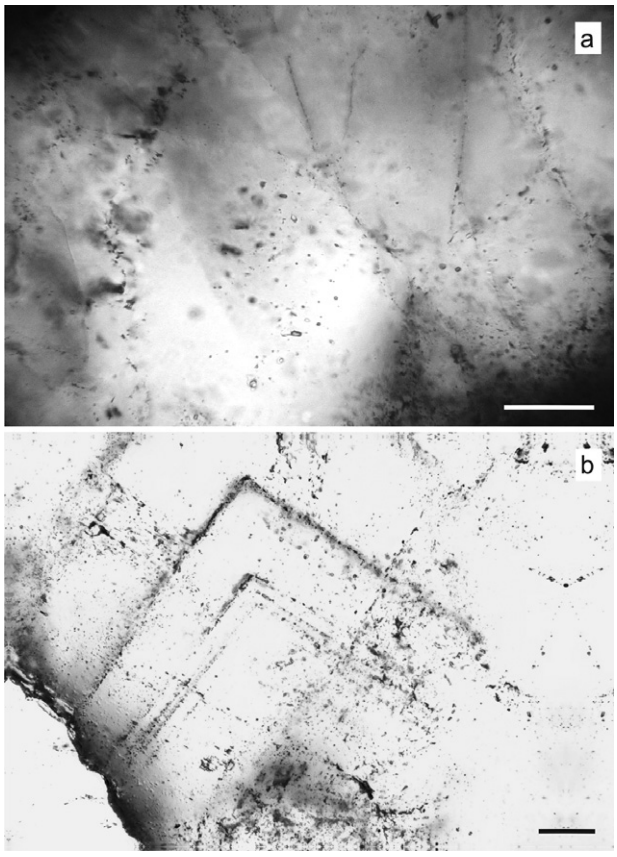

Fig. 4 (a) Fluid inclusions in the center of a quartz crystal. (b) Fluid inclusions in growth zones of a quartz crystal. Bar scale = 50 μm.

4.2 Microthermometry

Ten samples, representing all stages of mineralization but VI, were analyzed. One hundred and twenty one melting temperatures and 82 homogenization temperatures were obtained in quartz and fluorite (Fig. 5). Petrographic evidence of boiling, related to bladed textures in quartz, was found in some FIAs from the stage IV, where volumetrically different relations in the vapor-liquid phases are present. In Stage II, adularia crystals and bladed quartz textures were found but no petrographic evidence of boiling was identified in their FIAs. The microthermometric data were summarized in Table 1.

Fluid inclusions in quartz samples have average salinities in the range of 2.57 to 4.96 wt% $NaCl_{equiv.}$ and average homogenization temperatures in the range of 224.6 to 286.9°C. The fluid inclusions in fluorite samples have lower values, the salinity ranges from 0.70 to 1.57 wt% $NaCl_{equiv.}$ and homogenization temperatures from 160.8 to 186.8°C.

4.3 Stable isotopes

As a complement, stable isotope studies were performed. The oxygen fractionation was analyzed from seven quartz samples and sulfur from two pyrite samples. Table 2 summarizes the details of the analyzed samples. The resulting $\delta^{18}O$ values in quartz samples from the mineralization stages II, III, IVa, IVb and V are in the range of 1.11 to 4.41‰, relative to VSMOW. Considering the average homogenization temperature of each stage of mineralization, the oxygen fractionation of the hydrothermal fluid in equilibrium with quartz when crystallizing, was calculated. The fractionation of the oxygen in the hydrothermal fluid is in the range of $\delta^{18}O_{H2O}$ = –6.92 to –3.08‰, which indicates domination of meteoric source for the water.

In order to identify the source of sulfur in the sulfides from the Don Sixto area, two pyrite samples were analyzed. The obtained $\delta^{34}S$ values were 2.37 and

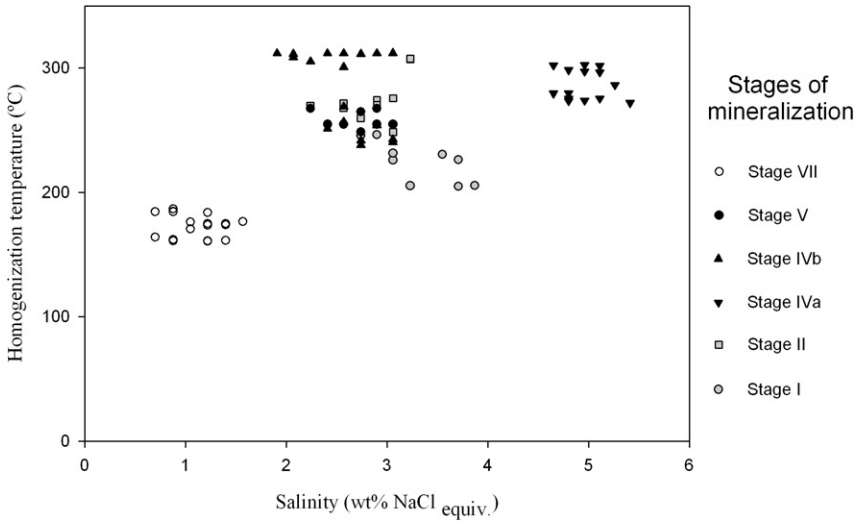

Fig. 5 Microthermometric results from the Don Sixto mining area.

Table 1 Microthermometric data from the Don Sixto mining project

Stages (mineral)	T_m (°C)			Salinity (wt% $NaCl_{equiv.}$)			T_h (°C)		
	Range	Avg.	*n*	Range	Avg.	*n*	Range	Avg.	*n*
I (Qz)	–1.2~–2.3	–1.8	16	2.07~3.87	3.06	16	204.8~246.2	224.6	9
II (Qz)	–1.2~–1.9	–1.6	14	2.07~3.23	2.74	14	248.7~307.6	274.7	11
III (Qz)	–1.3~–1.7	–1.5	10	2.24~2.90	2.57	10	—	—	—
IV a (Qz)	–2.8~–3.3	–3.0	23	4.65~5.41	4.96	23	272.2~302.7	286.9	14
IV b (Qz)	–1.1~–1.8	–1.5	29	1.91~3.06	2.57	29	238.2~312.0	286.5	21
V (Qz)	–1.3~–1.8	–1.6	9	2.24~3.06	2.74	9	248.7~267.6	258.1	9
VII (Fl)	–0.4~–0.9	–0.6	20	0.70~1.57	1.05	20	160.8~186.8	173.1	18

T_m, melting temperature; T_h, homogenization temperature; Avg., average; *n*, number of fluid inclusions; Qz, quartz; Fl, fluorite.

Table 2 Isotopic fractionation of oxygen and sulfur

Mineralizing stages	Prospect	Mineral sample	T_h Avg. (°C)	$\delta\,^{18}O_{Qz} \pm SD$	$\delta\,^{34}S_{py}$ (‰)	$\delta\,^{18}O_{H2O}$ (‰)	$\delta\,^{34}S_{H2S}$ (‰)
II	Luna	Qz	274.7	3.63 ± 0.04	—	–4.30	—
III	Cuello	Qz	—	1.82 ± 0.05	—	—	—
III OM	Mandíbula	Qz	—	2.51 ± 0.05	—	—	—
IV a	Luna	Qz	286.9	1.11 ± 0.01	—	–6.37	—
IV a	Cuello	Py	286.9	—	2.37	—	1.09
IV b	Luna	Qz	286.5	4.41 ± 0.05	—	–3.08	—
V	Cuello	Qz	258.1	1.68 ± 0.02	—	–6.92	—
V	Mandíbula	Qz	258.1	3.74 ± 0.03	—	–4.86	—
VI	Cuello	Py	—	—	1.77	—	—

Avg. (°C), average temperature; ± SD, standard deviation; Qz, quartz; Py, pyrite.

1.77‰, relative to VCDT, for the stages of mineralization IVa and VI respectively. Considering the homogenization temperature of the stage IVa (286.9°C), the calculated $\delta^{34}S_{H2S}$ value was 1.09‰; when plotting this result in relation to the different sulfur reservoirs it seems impossible to define a single source for this element.

5. Discussion and conclusions

Quartz is a dominant gangue mineral in hydrothermal veins and is typically the only phase deposited throughout the life span of the hydrothermal system; the characteristics of this mineral might reflect differing hydrothermal conditions during vein growth,

including those which favor gold mineralization (Dong *et al*., 1995).

In the Don Sixto area quartz is dominant, while adularia and fluorite are less frequent. The most represented textures in the quartz veins, besides massive, are crustiform, and comb, and zoned, that might be the result of episodic pressure release, and slow changing conditions during crystal growth, respectively (Dong *et al*., 1995). Bladed quartz, also found in other low sulfidation epithermal gold deposits (i.e. Etoh *et al*., 2002) is present in Stages II and IV and is assumed to be related to the dissolution of calcite blades and pseudomorphic replacement when the fluids cool further (Dong *et al*., 1995).

Even though the presence of adularia in rhombic to sub-rhombic crystals and as pseudo-acicular aggregates in bladed replacement textures, were found in Stage II, no petrographic evidence of boiling was observed in their quartz fluid inclusions and no mineralization is related with this stage. This lack of significant precious metal mineralization might indicate either that the hydrothermal fluid was barren, or that the conditions of precipitations were not met; laser ablation analyses will be performed to evaluate this last interpretation. On the other hand, in Stage IV, bladed quartz samples have coexisting liquid-rich and vapor-rich fluid inclusions indicating the fluid boiling. The textural and petrographic evidence indicate that the precious metal mineralization was caused by fluid boiling that mainly occurred at this stage in the Don Sixto area.

The isotope study was not performed at submillimeter scale (i.e. Hayashi *et al*., 2000, 2001), due to the deposit shape (scattered outcrops) and analytical limitations. The oxygen fractionation was analyzed in quartz samples from Stages II, III, III-OM, IVa, IVb and V and the $\delta^{18}O_{Qz}$ values are in the range of 1.11 to 4.41‰, relative to VSMOW. Taylor (1997) indicated that $\delta^{18}O_{H2O}$ values in the range of –7 to +2‰ leave no doubt that the ore fluid at Creede (CO, USA) had a meteoric origin. The calculated $\delta^{18}O$ for the fluids in equilibrium with the Don Sixto quartz veins are in the range of $\delta^{18}O_{H2O}$ = –6.92 to –3.08‰, which is coherent with a meteoric water source and values obtained in epithermal systems elsewhere. Considering the observations of Truesdell *et al*., (1977) and Scott and Watanabe (1998), the oxygen enrichment observed in the $\delta^{18}O_{H2O}$ values from –6.37 to –3.08‰, for Stage IVa and IVb, respectively, may be ascribed to a boiling process. The results would also match the detailed observations of Hayashi *et al*., (2000, 2001) who demonstrated that the formation of epithermal veins is the result of intermittent opening of the system associated with boiling and allowing the interaction of mineralizing fluids with meteoric waters, leading to the precipitation of the precious metals. The possibility of a magmatic input, as suggested by some authors for both, active hydrothermal systems (i.e. Hedenquist & Aoki, 1991; Seki, 1991; Giggenbach, 1992) and mineralized epithermal systems (i.e. O'Neil & Silberman, 1974; Matsuhisa & Aoki, 1994) is still considered as a possibility, and further investigations are planned in that regard.

The analytical results obtained for $\delta^{34}S_{py}$ are 2.37 and 1.77‰, relative to VCDT, and the calculated isotopic fractionation of sulfur in the hydrothermal fluid is $\delta^{34}S_{H2S}$ = 1.09‰, these results might be coherent with a volcanic source, potentially the acid volcanic rocks of the Choique Mahuida Formation, with a possible contribution from the sedimentary rocks of the Agua Escondida Formation.

Acknowledgments

The authors are grateful to CONICET for the financial support through the grants PIP 5907 and 100857 and to Extorre Gold Mines Limited for giving access to the deposit, contributing with information and funding stable isotope analyses. ACML is also grateful to CONICET for the fellowships awarded to her. R. Lira gave access to the Fluid-Inc stage in the Alfred Stelzner Museum (National University of Córdoba, Argentina). The authors are grateful for the thorough and constructive review of the manuscript by Hiroyasu Murakami and for the editorial suggestions and corrections made by the Editor, Yasushi Watanabe.

References

Beaudoin, G. and Therrien, P. (1999-2012) alphadelta: calculateur du fractionnement des isotopes stables (Stable Isotope Fractionation Calculator). Département de géologie et de génie géologique, Université Laval, Québec, Canada. [Cited 1 Oct 2012.] Available from URL: http://www2.ggl.ulaval.ca/cgi-bin/isotope/generisotope.cgi

Bodnar, R. J. (2003) Re-equilibration of fluid inclusions. *In* Samson, J., Anderson, A. and Marshall, D. (eds.) Fluid inclusions: analysis and interpretation. Mineralogical Association of Canada, Ottawa, 213–230.

Bodnar, R. J., Reynolds, T. J. and Kuehn, C. A. (1985) Fluid-inclusion systematics in epithermal systems. *In* Berger, B. R. and Bethke, P. M. (eds.) Reviews in economic geology, geology and geochemistry of epithermal systems. Society of Economic Geologists, Littleton, CO, 73–97.

Bodnar, R. J. and Vityk, M. O. (1994) Interpretation of microthermometric data for H_2O-NaCl fluid inclusions. *In* De Vivo, B. and Frezzotti, M. L. (eds.) Fluid inclusions in minerals, methods and applications. Virginia Tech, Blacksburg, VA, 117–130.

Carpio, F., Mallimacci, H., Rubinstein, N., Salvarredi, J., Sepúlveda, E., Centeno, R., Rosas, M. and Vargas, D. (2001) Metalogenia del Bloque de San Rafael, Mendoza. SEGEMAR, Buenos Aires, 1–109.

Clayton, R. N. and Mayeda, T. K. (1963) The use of bromine pentafluoride in the extraction of oxygen from oxides and silicates for isotopic analysis. Geochim. Cosmochim. Acta, 27, 43–52.

Delendatti, G. L. (2005) La Cabeza: un depósito epitermal aurífero de baja sulfuración en el Bloque de San Rafael, Mendoza, Argentina. Actas del VIII Congreso Argentino de Geología Económica, Buenos Aires, 199–206.

Delendatti, G. L. and Williams, M. T. (2007) Don Sixto project, solid geology 1225m RL. Unpubl. Internal Report, Exeter Resource Corporation, 1p.

Dong, G. and Morrison, G. W. (1995) Adularia in epithermal veins, Queensland: morphology, structural state and origin. Mineral. Deposita, 30, 11–19.

Dong, G., Morrison, G. W. and Jaireth, S. (1995) Quartz textures in epithermal veins, Queensland-classification, origin, and implication. Econ. Geol., 90, 1841–1856.

Etoh, J., Izawa, E., Watanabe, K., Taguchi, S. and Sekine, R. (2002) Bladed quartz and its relationship to gold mineralization in the Hishikari low-sulfidation epithermal gold deposit, Japan. Econ. Geol., 97, 1841–1851.

Giggenbach, W. F. (1992) Isotopic shifts in waters from geothermal and volcanic systems along convergent plate boundaries and their origin. Earth Planet. Sci. Lett., 113, 495–510.

Godeas, M. and Rubinstein, N. (2004) Buddingtonita en el depósito epitermal El Pantanito, Mendoza. Actas del VII Congreso de Mineralogía y Metalogenia, Río Cuarto, 61–62.

Hayashi, K., Maruyama, T. and Satoh, H. (2000) Submillimeter scale variation of oxygen isotope of vein quartz at the Hishikari deposit, Japan. Resour. Geol., 50, 141–150.

Hayashi, K.-I., Maruyama, T. and Satoh, H. (2001) Precipitation of gold in a low-sulfidation epithermal gold deposit: insights from a submillimeter-scale oxygen isotope analysis of vein quartz. Econ. Geol., 96, 211–216.

Hedenquist, J. W. and Aoki, M. (1991) Meteoric interaction with magmatic discharges in Japan and the significance for mineralization. Geology, 19, 1041–1044.

Henley, R. W. (1985) The geothermal framework of epithermal deposits. *In* Berger, B. R. and Bethke, P. M. (eds.) Reviews in economic geology, geology and geochemistry of epithermal systems. Society of Economic Geologists, Littleton, CO, 1–24.

Kay, S. M., Ramos, V. A., Mpodozis, C. and Sruoga, P. (1989) Late Paleozoic to Jurassic silicic magmatism at the Gondwanaland margin: analogy to the Middle Proterozoic in north America? Geology, 17, 324–328.

Kleiman, L. E. (1993) El volcanismo Permo-Triásico y Triásico del Bloque de San Rafael (provincia de Mendoza): su potencial uranífero. Actas del XII Congreso Geológico Argentino y II Congreso de Exploración de Hidrocarburos, Mendoza, 284–293.

Kleiman, L. E. and Japas, M. S. (2009) The Choiyoi volcanic province at 34°S-36°S (San Rafael, Mendoza, Argentina): implications for the Late Paleozoic evolution of the southwestern margin of Gondwana. Tectonophysics, 473, 283–299.

Llambías, E. J. (1999) Las rocas ígneas gondwánicas. 1. El magmatismo gondwánico durante el Paleozoico superior-Triásico. *In* Caminos, E. (ed.) Geología argentina. Instituto de Geología y Recursos Minerales, Buenos Aires, Anales 29, 349–376.

Llambías, E. J., Kleiman, L. E. and Salvarredi, J. A. (1993) El magmatismo gondwánico. *In* Ramos, V. A. (ed.) Geología y Recurso Naturales de Mendoza, Relatorio del XII Congreso Geológico Argentino y II Congreso de Exploración de Hidrocarburos, Mendoza, 53–64.

Martin, M. W., Clavero, J. and Mpodozis, C. (1999) Late Paleozoic to Early Jurassic tectonic development of the high Andean Principal Cordillera, El Indio Region, Chile (29–30°S). J. S. Am. Earth Sci., 12, 33–49.

Matsuhisa, Y. and Aoki, M. (1994) Temperature and oxygen isotope variations during formation of the Hishikari epithermal gold-silver veins, southern Kyushu, Japan. Econ. Geol., 89, 1608–1613.

Mugas Lobos, A. C. (2012) Estudios mineralógicos, geoquímicos y metalogenéticos en el proyecto minero Don Sixto (ex La Cabeza), Mendoza, Argentina. Unpubl. PhD thesis, Universidad Nacional de Córdoba, Córdoba, 289 pp.

Mugas Lobos, A. C., Márquez-Zavalía, M. F. and Galliski, M. A. (2010) Petrografía y geoquímica de las rocas gondwánicas del proyecto minero Don Sixto, Mendoza. Rev. Asoc. Geol. Argent., 67, 392–402.

Mugas Lobos, A. C., Márquez-Zavalía, M. F. and Galliski, M. A. (2011) Selenium and precious metal-bearing minerals at Don Sixto mining project, Mendoza, Argentina. SGA 2011: let's talk ore deposits, 708–710.

Mugas Lobos, A. C., Márquez-Zavalía, M. F. and Galliski, M. A. (2012a) Minerales de mena del depósito epitermal de baja sulfuración Don Sixto, Mendoza. Rev. Asoc. Geol. Argent., 69, 3–12.

Mugas Lobos, A. C., Ordoñez, M., Márquez-Zavalía, M. F. and Galliski, M. A. (2012b) Spectral identification of buddingtonite and associated minerals at Don Sixto, a low sulfidation Au–Ag deposit. Hedenquist, J and Fontboté, L. (Comp.); Brandt, C. (ed.) SEG Conference 2012, Integrated Exploration and Ore Deposits, Lima, Perú, 1–3.

Narciso, V., Zanettini, J. C., Santamaría, G. and Mallimacci, H. S. (2007) Hoja geológica 3769-II, Agua Escondida, provincias de Mendoza y La Pampa, 2nd edn. Instituto de Geología y Recursos Minerales, SEGEMAR, Buenos Aires, Boletín 300: 54 pp.

O'Neil, J. R. and Silberman, M. L. (1974) Stable isotope relations in epithermal Au–Ag deposits. Econ. Geol., 69, 902–909.

Ohmoto, H. and Rye, R. O. (1979) Isotope of sulfur and carbon. *In* Barnes, H. L. (ed.) Geochemistry of hydrothermal deposits, 2nd edn. John Wiley & Sons, New York, 509–567.

Ramos, V. A. (1999) Ciclos orogénicos y evolución tectónica. *In* Zappettini, E. O. (ed.) Recursos Minerales de la República Argentina. SEGEMAR, Buenos Aires, Anales 35, 29–49.

Roedder, E. (1984) Fluid inclusions. Mineralogical Society of America, Reviews in Mineralogy, 12: 644 pp.

Rubinstein, N., Carpio, F. and Mallimacci, H. (2001) El depósito epitermal El Pantanito, provincia de Mendoza. Rev. Inst. Geol. Min. UNJU, 14, 59–61.

Rubinstein, N. and Gargiulo, M. F. (2005) Análisis textural de cuarzo hidrotermal del depósito El Pantanito, provincia de Mendoza: nuevos aportes sobre su génesis. Rev. Asoc. Geol. Argent., 60, 96–103.

Scott, A.-M. and Watanabe, Y. (1998) "Extreme boiling" model for variable salinity of the Hokko low-sulfidation epithermal Au prospect, southwestern Hokkaido, Japan. Mineralium Deposita, 33, 568–578.

Seki, Y. (1991) The physical and chemical structure of the Okuaizu geothermal system, Japan. Geochem. J., 25, 245–265.

Stipanicic, P. N., Rodrigo, F. O. L. and Martínez, C. G. (1968) Las formaciones presenonianas en el denominado Macizo Nordpatagónico y regiones adyacentes. Rev. Asoc. Geol. Argent., 23, 67–98.

Taylor, H. P. Jr (1997) Oxygen and hydrogen isotope relationships in hydrothermal mineral deposits. *In* Barnes, H. L. (ed.) Geochemistry of hydrothermal ore deposits, 3rd edn. John Wiley & Sons, New York, 229–302.

Truesdell, A. H., Nathenson, M. and Rye, R. O. (1977) The effects of subsurface boiling and dilution on the isotopic compositions of Yellowstone thermal waters. J. Geophys. Res., 82, 3694–3704.

Van der Heyden, A., Yeo, W., Delendatti, G. L. A. and Williams, M. T. (2007) Technical report: 2007 revised resource estimation, Don Sixto Gold Project, Mendoza province, Argentina. Exeter Resource Corporation, Vancouver, Canada, 638 pp.

Whitney, D. L. and Evans, B. W. (2010) Abbreviations for names of rock-forming minerals. Am. Mineral., 95, 185–187.

Zappettini, E. O. (1999) Evolución geotectónica y metalogénesis de Argentina. *In* Zappettini, E. O. (ed.) Recursos Minerales de la República Argentina. SEGEMAR, Buenos Aires, Anales 35, 51–73.

Zheng, Y. F. (1993) Calculation of oxygen isotope fractionation in anhydrous silicate minerals. Geochim. Cosmochim. Acta, 57, 1079–1091.